Friction Analysis and Modelling of a Novel Stepped Rotary Flow Control Valve

Karem Abuowda, Ivan Okhotnikov, and Siamak Noroozi
PhD researcher at Bournemouth University
Poole, Dorset, BH12 5BB, UK
kabuowda@bournemouth.ac.uk

Phil Godfrey
Engineering Director at Hydreco Hydraulics Ltd
Poole, Dorset, BH16 5SL, UK

Abstract

High flow rate control is very important for different applications ranging from constructional, industrial, military and aerospace. Generally, hydraulic control relies on different types of valves. For example, poppet and spool valves have been implemented in Independent Metering (IM) system which is usually installed in mobile hydraulic machines such as excavators. Recently, a novel rotary flow control orifice has been developed to design a control valve for high flow rate applications, and a stepper motor was selected as the main actuator for this orifice to grant more accuracy and controllability. The coupling between these two main components requires analysis of the internal dynamical interactions and their effect on the performance. Friction torque is an important parameter to be considered in this design. The paper includes analysis and modelling of the friction torque in the orifice which affects the coupling, also it contains a model validation and evaluation resulted from friction practical measurements.

1. Introduction

Hydraulic systems have been widely used due to their significant properties such as high power density, flexibility, and high stiffness[1]. They can be used in military, aerospace, industrial and earth moving machines. Different systems were improved to enhance the performance of hydraulic systems. Independent Metering (IM) is an important technique invented for more than 40 years ago[2]. Many flow control valves have been evolved to perform the role of IM. These valves suffer from low controllability which affects the machine performance. Recently, a new rotary flow control orifice has been invented by cooperation work between Bournemouth University and HYRECO Hydraulic Ltd aiming to improve the controllability of mobile hydraulic machinery[3]. A hybrid bipolar stepper motor was selected to be the main actuator for this orifice to improve the controllability and reduce the size of the valve. Analysis of the coupling between the two main components is necessary to obtain good performance. One of the main parameters to consider during coupling design is the friction torque between the orifice parts because the friction deteriorates the control system performance from high tracking error, settling time and stick-slip phenomena. This torque should be restricted by the stepper motor holding torque to achieve a successful and controllable coupling. Also modelling the friction in this part is necessary to perform

different advanced control algorithms. So, the main aim of this paper is to investigate the friction in the rotary orifice and determine a suitable model for this parameter.

In literature, a comparative study for three friction models which are the steady-state friction model, the LuGre and the new modified LuGre was performed to determine the suitable model for electrohydraulic servo system. The research concluded by experimentation that the new LuGre model able to presents the friction accurate[4]. The drift in the different friction models was evaluated to outcome that the improved LuGre model and the Ferretti are able to eliminate the drift in hydraulic servo system[5]. Pressure difference in hydraulic cylinder produces a variation between the friction model and the real measurements. The study indicated that hysteresis behaviour is highly affected by the pressure drop[6]. In a hydraulic cylinder, the friction is based on many parameters such as position and velocity, and a stribeck curve was used to model a servo hydraulic system[7]. As the friction is nonlinear and depends on the system construction parameters such type, shape and pressure difference etc, so this rotary orifice requires analysis and friction model study which was performed during through this research. This study is organised as follows: in Section 2, the valve work principle and work construction are included. In Section 3, Friction analysis and modelling brief review. In Section 4, the rotary orifice modelling and simulation using luGre model is covered. The model validation is in Section 5, and the conclusion is in Section 6.

2.   The stepped rotary valve construction and main working principle

The rotary flow control valve considered in this research is shown in Figure 1. The flow is controlled by the position of the rotor in the stepper motor. Figure 2 shows the schematic construction of the motor and the orifice. When the driving circuit of the motor starts feeding current into the coils, an electromagnetic force is produced in the stators[8]. The force rotates the stepper rotator which is connected to the valve spool. Consequently, the opening area of the orifice is changed. Figure 3 illustrates the relation between the rotation angle and the produced flow under different pressure drops.
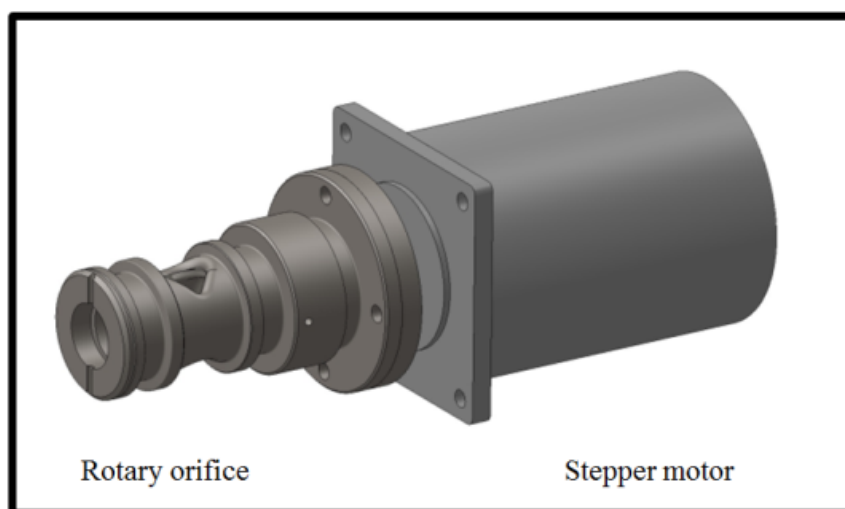

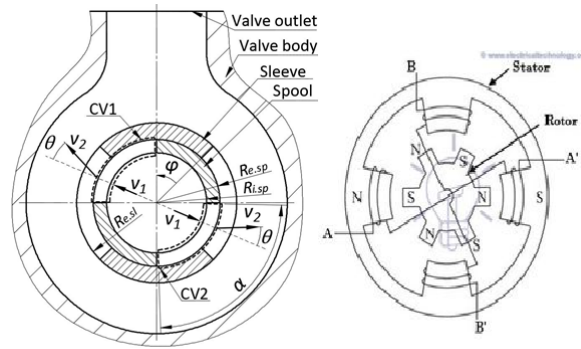**Figure 1 The novel stepped rotary flow control valve.**

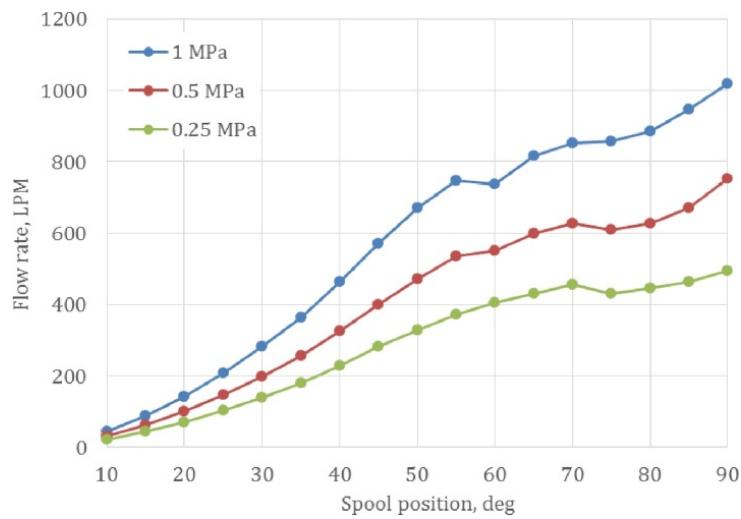**Figure 2 Construction of the two parts of the valve which are the rotary orifice and the stepper motor**

Figure 3 The fluid flow regime of the rotary orifice related to the opening areas with different pressure drops [3].

3. Friction Analysis and Modelling

By considering a simple mechanical system which contains a small box moving on a surface as showing in Figure 4, two main friction regimes can be detected which are pre-sliding regime and the gross sliding regime as illustrated in Figure 5. In the first regime which is the pre-sliding, the friction force depends on the displacement rather than velocity. This is due to the elasto-plastically deformation of the asperities junctions. Increasing the displacement lead to break more junctions and they have less time to reform which leads into the gross sliding regime. In this reign, the friction force is a function of velocity as the asperity junction is continually forming and breaking. Different factors affect the transition between the two regimes which is a critical point, such as velocity, displacement rate and the acceleration[9].
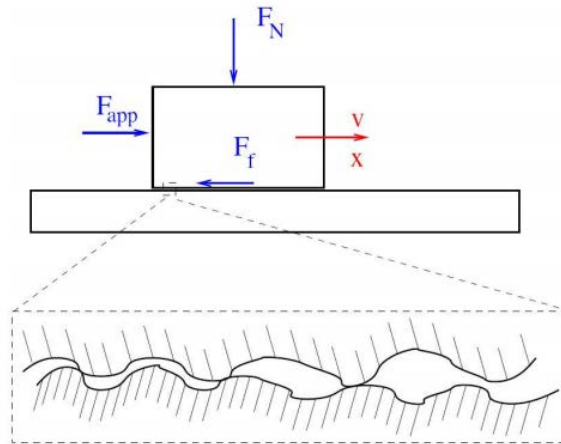
Figure 4 A simple configuration illustrates the friction where Fapp is the applied force, Fn is the body weight force, Ff is the friction force[9].
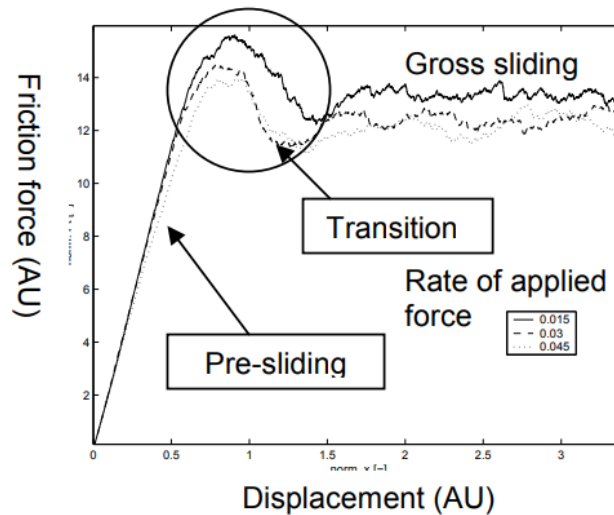

Figure 5 illustrates the two friction regimes and the transition between them [9].

Different models can be used to represents the friction between two surfaces. They are Dahl model, LuGre Model and Leuven Model. Dahl model of friction is one of the earliest models and it was developed for aerospace industry[10]. It's a simple hysteresis function. The Dahl model equation as obtained from[9] is

$$\frac{dF}{dx} = \sigma_0\, sgn\left(1 - sgn(v)\frac{F}{Fc}\right) \qquad (1)$$

Where F is the friction force [N], x is the body displacement [m], v is the sliding velocity [m/s], σ_0 is the asperity stiffness [N/m], and Fc is the coulomb friction.

The LurGe model which is a developed version of the Dahl one includes a representation of hysteresis shape, Stibeck curve, and viscous damping coefficient. It's main equation as obtained from[10] is

$$\begin{cases} F = \sigma_0 z + \sigma_1 \dot{z} + \sigma_2 \omega \\ \dot{z} = \omega - \dfrac{\sigma_0 |\omega|}{g(\omega)} z \\ g(\omega) = Tc + (Ts - Tc)\exp(-(\omega/\omega_s))^\delta \end{cases} \qquad (2)$$

Where F is the friction force, $g(\omega)$ is Stribeck curve in a function of sliding velocity, σ_0 is the bristle stiffness, σ_1 is the damping coefficient [Ns/m], σ_2 is the viscous coefficient [N/m], Ts is the friction torque [N], Tc is the Coulomb friction torque [N], and δ is the friction coefficient.

Leuven analysed the behaviour of the presiding regime as a hysteresis function of the position, with non-local memory. The obtained model by Leuven represents insertion of this specific behaviour into LuGre model[11]. A mathematical representation of this model can be

$$\begin{cases} F = F_h(z) + \sigma_1 \dfrac{dz}{dt} + \sigma_2 \omega \\ \dfrac{dz}{dt} = \omega\left(1 - sgn\left(\dfrac{F_h(z)}{g(\omega)}\right)\left|\dfrac{F_h(z)}{g(\omega)}\right|^\delta\right) \\ g(\omega) = Tc + (Ts - Tc)\exp(-(\omega/\omega_s))^\delta \end{cases} \qquad (3)$$

Where $F_h(z)$ is a nonlinear hysteresis force function which can be represented by Maxwell slip model that is included in reference[12].

4. The Rotary Orifice Friction Modelling and simulation using LuGre model

The LuGre model [13 14)] has been selected as it provides a reasonable compromise between model complexity influencing on the computational time needed to implement the model and accuracy of friction behaviour modelling or completeness of phenomena included in the model. It has been also proved to be suitable for a state-space approach in dynamic analysis [15].

As indicated in Figure 2, the spool and the sleeve are concentric parts with a small radial clearance between them; the viscous frictional torque acting on the spool from the annular liquid volume at motion in the clearance can be considered as laminar Couette flow and calculated according to Newton's law of viscosity:

$$\sigma_2 \omega = \tau A_{sp} R_{e.sp} = \frac{\mu R_{e.sp}^2 A_{sp} \omega}{\delta}. \qquad (4)$$

Here τ is shear stress, μ – the dynamic viscosity coefficient of the fluid, A_{sp} – the total area of the spool external cylinder subjected to the shear stress in the annual gap with a clearance

$$\delta = R_{i.sl} - R_{e.sp}. \qquad (5)$$

Here $R_{i.sl}$ and $R_{e.sp}$ are the inner sleeve and the external spool radii respectively.

Viscous shear stress τ acts on the spool cylindrical surfaces in the annular gap with the clearance δ. The spool external cylinder houses two sets of balancing grooves, which prevent formthe ation of a hydraulic lock and centre the spool concentrically inside the sleeve [16], as well as two throttling orifices. These regions do not contribute to the viscous friction torque on the spool since the radial distance from the spool to the sleeve there is not equal to the clearance δ. Thus, the total area of interest is

$$A_{sp} = 2\pi R_{e.sp}(L - nw) - 2A_{sp.op}. \tag{6}$$

This expression includes the length of the spool located inside the sleeve L; n, w are the total number and the width of the balancing grooves respectively.

The solid-to-solid sliding Coulomb friction in the case of the considered design takes place between the spool and elastomer O-ring seals and back-up rings. Sealing between moving mechanical parts is ensured by squeezed elastomer and plastic back-up rings during assembly. This squeeze produces the drag friction torque from an elastomer ring on the sealant part[17].

To quantify parameters of the friction model, one needs to consider every source of static friction. As for the rotary valve we study, static friction acting on the spool is a sum of friction forces generated from every O-ring and backup ring contacting with the spool.

In the applied method of estimation, the dry friction torque from sealing, running friction is estimated at first via Stribeck diagrams for used oil pressure range and O-rings design. The break-out friction is derived from the running one.

The Coulomb (or running) friction torque T_C is defined through stabilized (running) friction force F_C, which depends on the friction coefficient and the force F_t generated by the squeezed sealing ring after assembly compression and application of oil pressure on it[18].

$$T_C = F_C R_{sp} = \mu_w F_t R_{sp} \tag{7}$$

In this expression R_{sp} is a spool shaft radius, on which the contact between the spool and the sealing ring takes place. In the design of the considered valve, all seals are of rod type, i.e. sealing rings are housed in parts surrounding the spool; μ_w is the friction coefficient.

The stabilized expected friction force (at the middle of the spool stroke) may be determined as follows:

$$F_t = 2\pi R_{sp} b p_w, \tag{8}$$

where p_w is working, operating pressure, which can be considered for high-pressure hydraulic applications equal to the pressure difference between chambers separated by the sealing ring and b is the total compressed seal width.

For O-rings, the seal width b_o is approximated through its cross-section diameter d_2:

$$b_o = \sqrt{\frac{\pi d_2^2}{4}}. \tag{9}$$

The backup ring seal width is the same as the ring's width b_b [18] as its compression is negligible comparing to rubber seal's one. Thus, the total seal width is

$$b = b_o + b_b. \tag{10}$$

In case of application of O-rings with PTFE backup rings in high-pressure and low-speed conditions, the friction coefficient becomes mostly dependent on the working pressure. Taking the operating pressure p_w equal to 20 MPa, the friction coefficient is

$$\mu_w = \mu_{20} = 2.7 \cdot 10^{-2}. \tag{11}$$

The stiction friction can be considered proportional to the Coulomb friction force F_C with proportionality coefficient c, which represents the friction force hysteresis when the motion direction changes. The value of the change coefficient is taken equal to $c = 1.2$ at the relative linear velocity is in range fromthe 0.05 m/s to 0.3 m/s, i.e.

$$F_S = cF_C = 1.2F_C. \tag{12}$$

Figure 6 represents the model establishing using Simulink, and Figure 7 shows the performance of the friction model when a sine wave input 1Hz, represents the velocity and was applied to the model.
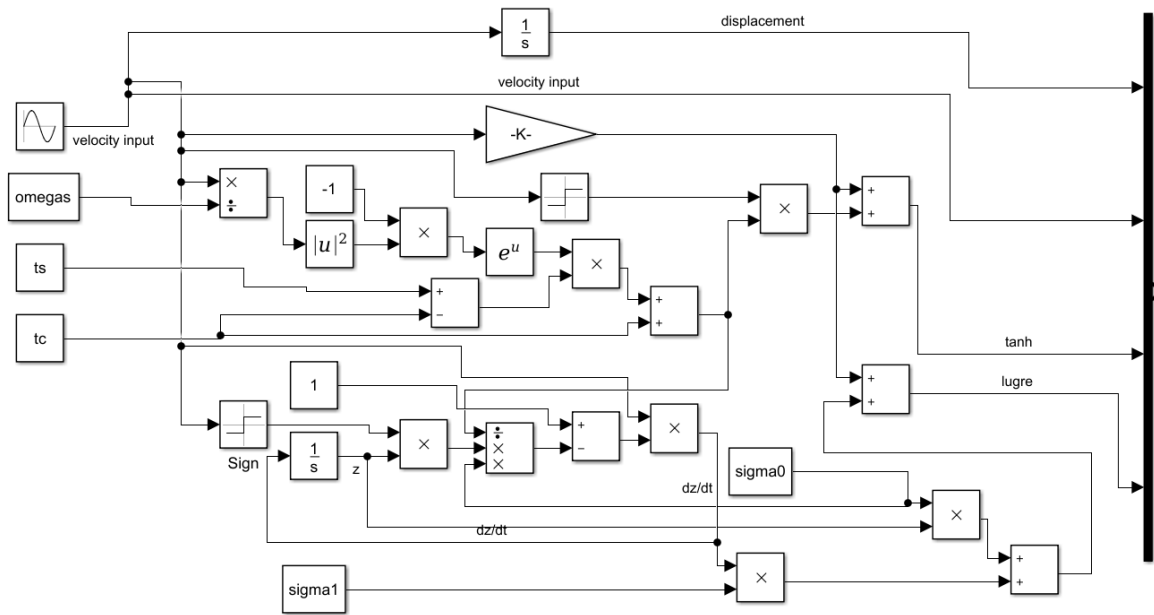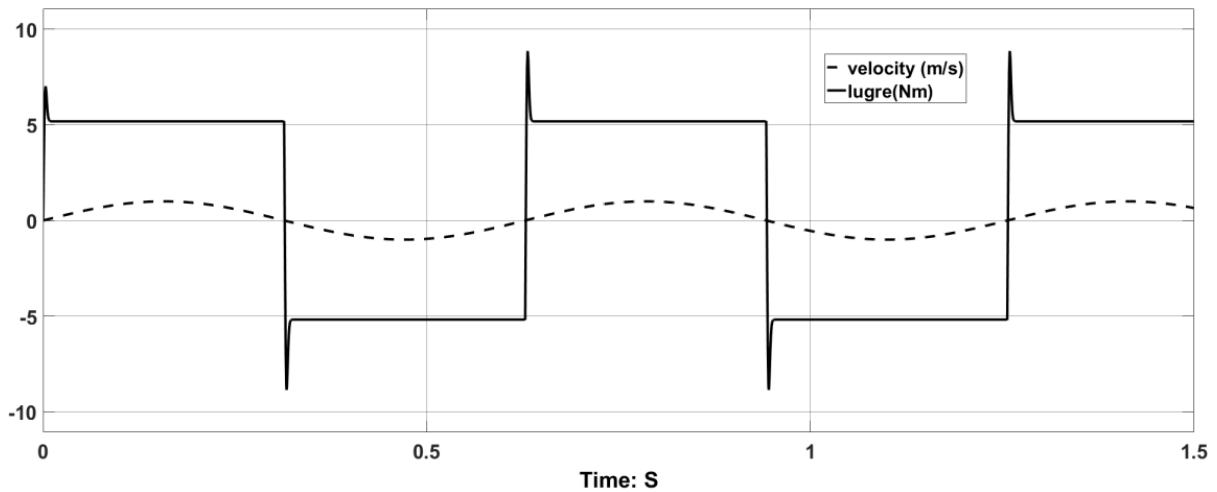

Figure 6 The friction model using Simulink.

Figure 7 The initial performance of the friction model.

5. Model Validation

Friction is an important parameter affecting the performance of the valve and the in the real implementation. A practical evaluation of this parameter is necessary to determine the suitable stepper motor as an actuator for the rotary orifice. As the valve orifice is in the early stage of testing, a static test has been performed to quantify the valve performance, and a test to quantify the friction parameters was executed. The test rig was attached with an advanced stepper motor and micro step driver as shown in Figure 6 and Figure 7. The attached motor is a 5 phases stepper motor with 0.72° step degree and 6 Nm holding torque. The driver is provided with a smooth driving function, which keeps the motor step size as small as possible, that is 0.0032°. Also, the stepper motor current is not affected by the division and stay stable all the time. The operation commands were sent from the control PC into the driver and the measurement PC was included to obtain the measurement signals and record them. Measurements captured for the friction during operations are shown in Figure 8 and Figure 9. As illustrated in these figures, the average of the friction torque is 1.5 Nm. The torque ripples value which appears when the valve starts moving is about 3 Nm. On the other hand, the friction testing results show that two factors Tc and Ts of the model should be modified. The new values are 2 and 3 instead of 5:17 and 6:213 are selected during simulation. Hence, the friction performance of the valve is illustrated in Figure 12.
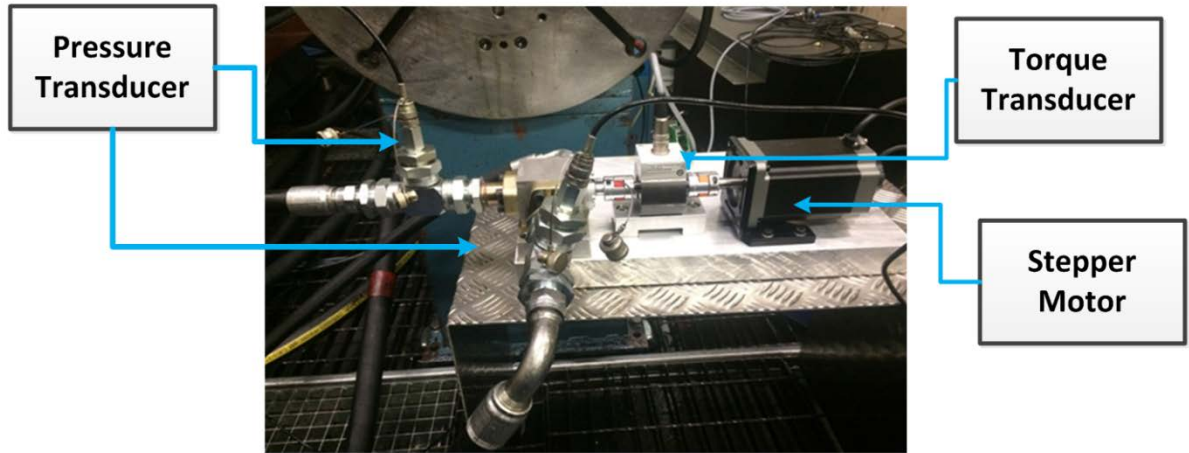
Figure 8 The test rig for the valve to determine the value to evaluate the value of the friction torque and validate the model.
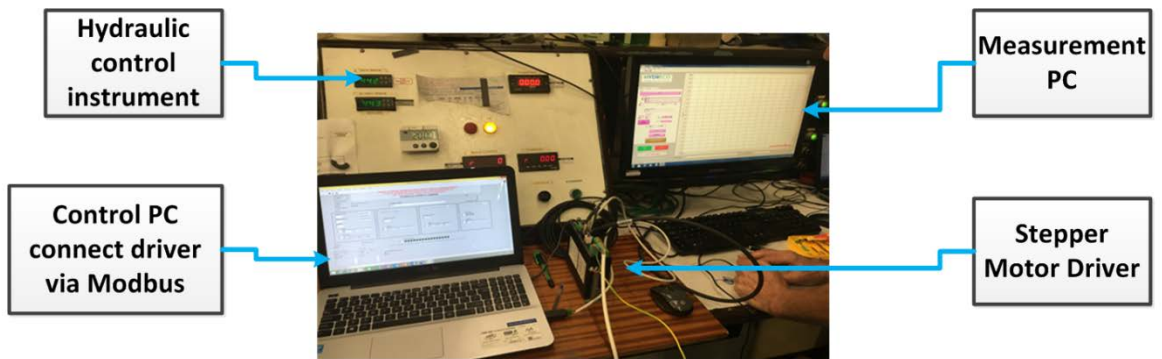

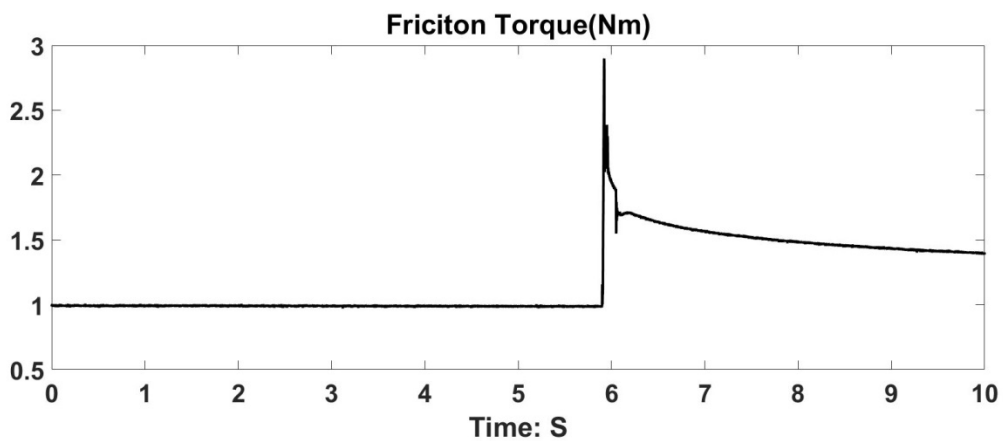**Figure 9 The measurement and the controller parts of the test rig.**

Figure 10 The rotary orifice friction when the valve rotates with switching frequency 200kHz.
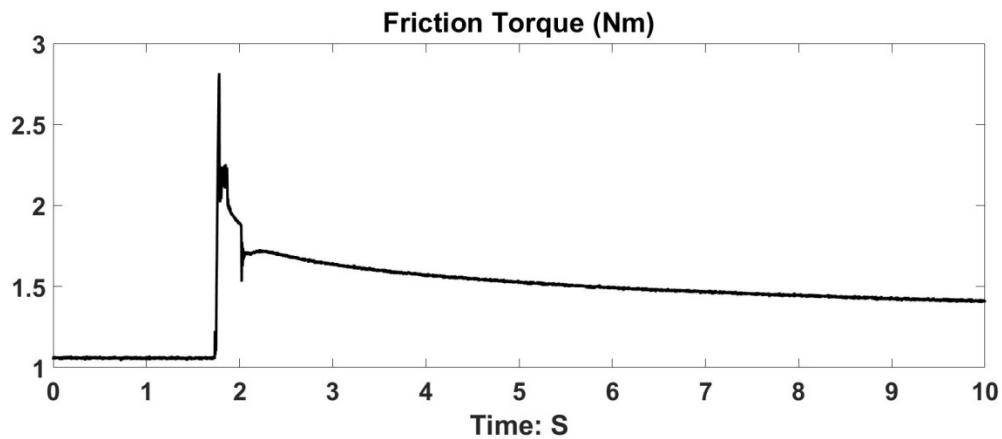
Figure 11 The rotary friction when the valve rotates with switching frequency 600KHz
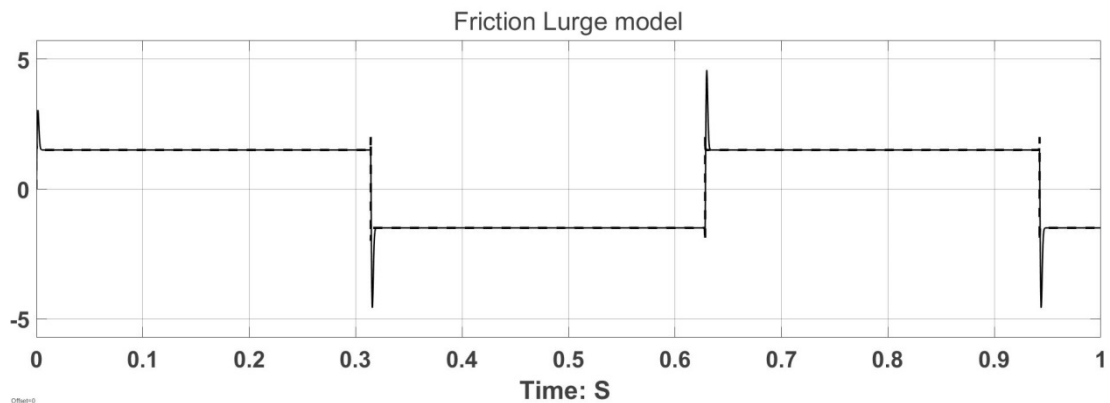

Figure 12 The friction model with changing the value of the coulomb friction and static friction in the model.

6. Conclusion

In this paper, the friction parameter in a novel hydraulic flow control orifice has been investigated to determine the value of the required torque from the valve actuator which is a stepper motor. Also, the dynamic friction model to be used for control algorithm development was identified. According to the modelling and simulation and practical model validation, the suitable model that represents the dynamic friction of this orifice is LuGre type. The maximum ripple friction torque is 3 Nm at the start of rotating, which represents a critical point in control design. The average of the friction torque is 1.5 Nm during operation. The values of the viscous friction and the coulomb friction have been modified to be 2 N and 3 N instead of 5:17 N and 6:213 N which were selected during simulation.

7. Appendix

Table 1 Parameters symbols and values

Parameter	Symbol	Value
Oil density	ρ	853
External diameter	m	0.0096
Internal diameter	m	0.0097
Spool opening window	m^2	$8.75e^{-5}$
Static friction	N	6.2153
Coulomb friction	N	5.179
Stribeck velocity	rad/sec	0.001
Bristle damping coefficient	N/s	316.277
Bristle stiffness	Ns/m	10^5
Viscous friction coefficient	N/m	0.4

References

1. Parr A. *Hydraulic and Pneumatics Atechnician's and Engineer's Guide*.; 1999.

2. Eriksson B. Mobile Fluid Power Systems Design with a Focus on Energy Efficiency. *Linköping Univ Electron Press*. 2010:77.

3. Okhotnikov I, Noroozi S, Sewell P, Godfrey P. Evaluation of steady flow torques and pressure losses in a rotary flow control valve by means of computational fluid dynamics. *Int J Heat Fluid Flow*. 2017;64:89-102. doi:10.1016/j.ijheatfluidflow.2017.02.005.

4. Yanada H, Khaing WH, Tran XB. Effect of Friction Model on Simulation of Hydraulic Actuator. 2014:175-180.

5. Yang J, Plummer A, Xue Y. Dynamic friction modelling without drift and its application in the simulation of a valve controlled hydraulic cylinder system . 1991.

6. Bo X, Hafizah N, Yanada H. Modeling of dynamic friction behaviors of hydraulic cylinders. *Mechatronics*. 2012;22(1):65-75. doi:10.1016/j.mechatronics.2011.11.009.

7. Essa M, Aboelela M, Ahmed M, Hassan M. Position control of hydraulic servo system using proportional-integral-derivative controller tuned by some evolutionary techniques. 2014;(November). doi:10.1177/1077546314551445.

8. Kenjo T. Stepping motors an their microprocessor controls. 1984:244. doi:10.1080/03043799508928291.

9. Al-bender F. FUNDAMENTALS OF FRICTION MODELING.

10. Piatkowski T. Dahl and LuGre dynamic friction models - The analysis of selected properties. *Mech Mach Theory*. 2014;73:91-100. doi:10.1016/j.mechmachtheory.2013.10.009.

11. Swevers J, Al-bender F, Ganseman CG, Prajogo T. An Integrated Friction Model Structure with Improved Presliding Behavior for Accurate Friction Compensation. 2000;45(4):675-686.

12. Lampaert V, Swevers J, Al-bender F. Modification of the Leuven Integrated Friction Model Structure. 2002;47(4):683-687.

13. Canudas de Wit C, Olsson H, Astrom KJ, Lischinsky P. A new model for control of systems with friction. *Autom Control IEEE Trans*. 1995;40(3):419-425. doi:10.1109/9.376053.

14. Åström KJ, Canudas-de-wit C. Revisting the LuGre Friction Model. *IEEE Control Syst Mag*. 2008;28(December):101-114. doi:10.1109/MCS.2008.929425.

15. Owen WS, Croft EA. The reduction of stick-slip friction in hydraulic actuators. *IEEE/ASME Trans Mechatronics*. 2003;8(3):362-371. doi:10.1109/TMECH.2003.816804.

16. Merritt HE. *Hydraulic Control Systems*. New York: John Wiley & Sons, Inc.; 1968. doi:10.1115/1.3601167.

17. Al-Ghathian, Faisal, Tarawneh, Muafag. Friction Forces in O-ring Sealing. *Am J Appl Sci*. 2005;2(3):626-632. doi:10.3844/ajassp.2005.626.632.

18. Bisztray-Balku S. Tribology of hydraulic seals for alternating motion. *Period Polytech Mech Eng*. 1995;39(3-4):225-246.